Journal of Applied Polymer Science

Preparation and Characterization of Poly(ethylene terephthalate) Copolyesters Modified with Sodium-5-Sulfo-Bis-(hydroxyethyl)-Isophthalate and Poly(ethylene glycol)

Ming-Liang Zhao,[1] Fa-Xue Li,[1] Jian-Yong Yu,[2] Xue-Li Wang[2]
[1]College of Textile, Donghua University, Shanghai 201620, China
[2]Modern Textile Institute, Donghua University, Shanghai 200051, China
Correspondence to: F. Li (E-mail: fxlee@dhu.edu.cn) or J. Yu (E-mail: yujy@dhu.edu.cn)

ABSTRACT: Two types of poly(ethylene terephthalate) (PET) copolyesters were successfully prepared with sodium-5-sulfo-bis-(hydroxyethyl)-isophthalate (SIPE) and poly(ethylene glycol) (PEG) units with different molecular weights named as cationic dyeable polyester and easy cationic dyeable polyester. Their chemical and crystalline structures were characterized by the nuclear magnetic resonance (NMR), wide angle X-ray diffraction (WAXD), and small angle X-ray scattering measurement, and their thermal properties were tested by differential scanning calorimetry and thermogravimetric analysis, respectively. NMR experimental results showed that the actual molar ratio of comonomers was basically consistent with the correlative feed ratio. WAXD results indicated that the crystalline structures of prepared copolyesters were similar to that of PET. Moreover, the glass transition temperature, melting temperature, and thermal degradation temperature were found to decrease with the reduction of the $\overline{M_n}$ of PEG units as the incorporation of lower $\overline{M_n}$ of PEG units brought more ether bonds into molecular chains, which increased the irregularity of molecular chain arrangement and led to lower crystallinity. In addition, because the incorporation of PEG units with lower molecular weight led to more ether bonds and hydroxyl end-groups in molecular chains, the value of contact angle of PET copolyesters dropped, manifesting PET copolyesters had better hydrophilicity with the decreasing molecular weight of PEG units.© 2013 Wiley Periodicals, Inc. J. Appl. Polym. Sci. **2014**, *131*, 39823.

KEYWORDS: X-ray; differential scanning calorimetry (DSC); thermogravimetric analysis (TGA); hydrophilic polymers; structure–property relations

Received 15 March 2013; accepted 6 August 2013
DOI: 10.1002/app.39823

INTRODUCTION

Poly(ethylene terephthalate) (PET) is widely used in many domains of synthetic fibers, liquid containers, thermoforming plastics, engineering resins, and textile and apparel industry[1–4] because of its superior properties such as better elasticity, higher strength, thermal stability, and other advantages.[5–7] However, some disadvantages of PET fibers such as low moisture regain, poor dyeability and antistatic property, rigid, and waxy handling[8–10] are mainly involved by the high regularity of molecular chains, high crystallinity, and low hydrophilicity,[11,12] which are hindering their further application in textile, fashion, and other industries.

As copolymerization is a very feasible and effective method to modify the chemical and physical properties of PET fibers, researches on copolymerization to improve properties of PET fibers have been carried out for decades of years. The cationic dyeable polyester (CDP) fibers, owning negative dye site (sulfonated group), were successfully prepared in 1960s.[13] CDP fibers can be dyed into bright and lively colors with cationic dyes, but high temperature and high pressure conditions are still necessary because of their high regularity and high crystallinity resulted from the existing of the rigid benzene ring structure in molecular chains and the ionic aggregates.[14,15] Moreover, the higher content of negative dye sites generally leads to higher melt viscosity of copolyesters, which will result in the next process of spinning difficultly to continue.

On the basis of CDP, easy cationic dyeable polyester (ECDP) was synthesized by incorporating PEG into CDP molecular chains. ECDP fibers can be dyed at normal pressure. Moreover, the hygroscopicity and soft handling of ECDP fibers are much better than those of CDP (or PET) fibers thanks to the increase of ether bonds and hydroxyl value from PEG units,[16] and the decrease of regularity of molecular chain arrangement that led to more amorphous regions in copolyesters. However, thermal properties of ECDP became worse than those of PET and CDP because of the incorporation of PEG molecular segments.[17]

Especially, the thermal properties would be obviously affected if the molecular weight of PEG blocked into ECDP polymer was too low and its content in the main chains was too high.

Some papers referred to the properties of CDP or ECDP.[5,16–18] However, to the best of our knowledge, no one, respectively, synthesized the PET, CDP, and PET-based copolyesters modified with sodium-5-sulfo-bis-(hydroxyethyl)-isophthalate (SIPE) and PEG units, and systematically characterized their structures and properties. Herein, in this study we first prepared the PET, CDP, and PET-based copolyesters modified with comonomers of SIPE and PEG with different molecular weights. The effects of molecular weights of PEG units on chemical structures, crystalline structures, thermal properties, and hydrophilicity of prepared copolyesters were mutually compared and elucidated in detail.

EXPERIMENTAL

Materials

CDP and ECDP samples were prepared with the following raw materials: purified terephthalate acid (PTA) supplied by Yangzi Petrochemical, China; ethylene glycol (EG) supplied by Yangzi Petrochemical, China; sodium-5-sulfo-bis-(hydroxyethyl)-isophthalate (SIPE) supplied by Yangzhou Huitong, China; poly (ethylene glycol) (PEG) with the number average molecular weight ($\overline{M_n}$) of 2000, 4000, 6000 (PEG2000, PEG4000, PEG6000) supplied by Honam Petrochemical, Korea.

Esterification and Polycondensation Process

Samples were successfully synthesized with direct esterification method, which is commonly used in PET synthesis nowadays. The synthesis was carried out in a 5l reactor. PTA and EG with the feed molar ratio of 1 : 1.3 were first added into the reactor. Meanwhile, the catalyst (EG antimony) and thermal stability agent (triphenyl phosphate) were together fed into it. During esterification process, the reaction temperature was kept at 235–245°C, and the esterification reaction continued for about 2–2.5 h. After the end of esterification reaction, SIPE (feed molar ratio of SIPE/PTA = 3/100) and PEG with different molecular weights (feed weight ratio of PEG/PTA = 10/100) were added into the reactor together for prepolycondensation for about 0.5 h. Subsequently, polycondensation reaction occurred at the temperature of 260–270°C for 2–2.5 h. Then chips of copolyesters were prepared successfully after discharging, granulating, and drying process. According to the added SIPE, PEG6000, PEG4000, and PEG2000 units, the relevant sample is designated as CDP, ECDP6, ECDP4, and ECDP2, respectively. Their corresponding intrinsic viscosity through Ubbelohde viscometer was determined to be 0.713, 0.765, 0.753, and 0.739 dL/g.

Measurements and Characterization

Nuclear Magnetic Resonance (^{1}H-NMR) experiment was carried out on the spectrometer named Avance 400 Bruker. About 6 mg sample was put into special sample tube, and completely dissolved in the solvent of deuterated trifluoroacetic acid (CF_3COOD).

Wide angle X-ray diffraction (WAXD) measurement was implemented on the instrument named D/Max-2550 PC. The power of the generator is 40 kV X 40 mA, and Nickel-filtered Cu K_α radiation (λ = 1.54 Å) is used. All samples were firstly crystallized at 130°C for 1 h under vacuum condition, and were carefully made into fine powder.

Small angle X-ray scattering (SAXS) measurement was executed on the instrument of small angle X-ray scattering beamline of Shanghai Synchrotron Radiation Facility. The distance between the sample and detector is 5 m, and the wavelength of X-ray is 1.24 Å. Before measurement, stripe specimens were first uniaxially stretched into different strains along axial direction on the tensile instrument at room temperature.

Differential Scanning Calorimetry (DSC) measurement was performed by using the instrument of NETZSCH DSC204F1 under nitrogen atmosphere. The sample was carefully cut into small chips, and weighted about 6 mg. The sample was first heated from ambient temperature to 280°C at the heating rate of 20°C/min, and then was gradually cooled to −20°C at the cooling rate of 10°C/min. Thereafter, the sample was reheated to 280°C at the heating rate of 10°C/min. The thermal properties in this study were determined by the second heating run.

Thermogravimetric analysis (TGA) measurement was executed through the NETZSCH TGA209F1 instrument under oxygen and nitrogen atmosphere, respectively. Under nitrogen atmosphere, 6 mg sample was gradually heated from 25°C to 600°C at the heating rate of 10°C/min, and the residues were naturally cooled to normal temperature. Under oxygen atmosphere, the heating and cooling process was same as the process under nitrogen atmosphere.

Contact angle measurement was conducted on the optical contact anglemeter of OCA15EC. Film specimens (0.1 mm in thickness) were prepared by compression molding of solid products at the temperature of about 20°C above the melting temperature of these copolyesters at 30 kg/cm^2 for 2 min, subsequently quenched into ice water. These prepared films were dried for 24 h at room temperature under vacuum atmosphere. Contact angles were evaluated on both sides of film with a 3.0 mL drop of distilled water for five times by the sessile drop method.

RESULTS AND DISCUSSION

The Chemical Structures and Compositions of CDP and ECDP Samples

^{1}H-NMR Analysis. Figure 1 shows the ^{1}H-NMR spectra of CDP, ECDP, and PET samples. It was distinctly revealed that differences in the chemical shifts of signals are resulted from H protons of PTA, EG, SIPE, and PEG units. **H1** and **H2** protons are aromatic ones that are consistent with the SIPE unit, and their chemical shifts are located at around 8.90 ppm.[19] Another aromatic protons of **H3** are derived from the PTA unit, and the corresponding chemical shifts are about 8.15 ppm.[20,21] The aliphatic **H4** protons originated from the EG unit display the chemical shifts of about 4.15 ppm.[22] Moreover, parts of **H4** protons have different chemical shifts and splitting peaks, attributed to the effects of the different sequences of PTA and SIPE units linked to the EG unit. Another aliphatic **H5** protons corresponding to the PEG units have the chemical shifts of about 3.85 ppm. In addition, **HX** and **HY** protons are aliphatic ones that are mostly attributed to the diethylene glycol (DEG) unit.

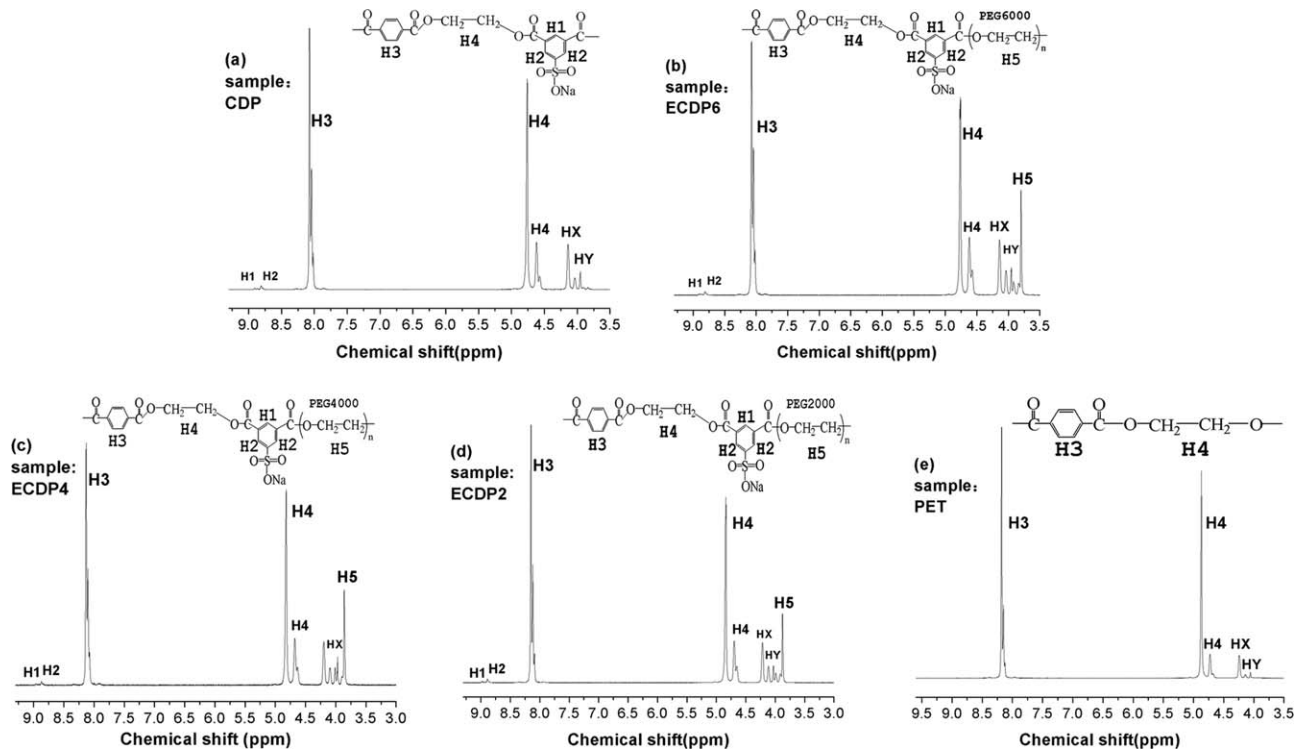

Figure 1. (a) ^{1}H-NMR spectra of the CDP sample. (b) ^{1}H-NMR spectra of the ECDP6 sample. (c) ^{1}H-NMR spectra of the ECDP4 sample. (d) ^{1}H-NMR spectra of the ECDP2 sample. (e) ^{1}H-NMR spectra of the PET sample.

It is well known that the production of the DEG by-product mostly is resulted from the chemical hydration reaction of EG, which frequently occurred during the synthesis of copolyesters under some conditions. Their chemical shifts lie in around 4.00 ppm.[23] Different chemical shifts and splitting peaks were clearly founded in H protons from the DEG unit, and the reason bears certain similarity to the above explanation of parts of **H4** protons from the EG unit.

Based on the chemical shifts in the ^{1}H-NMR spectra, the kind of chemical groups was able to be ascertained. By calculating the areas of resonance peaks, the relative molar ratio of different types of H protons and chemical groups could be obtained. Accordingly, the relative molar ratio of different units was determined. The results are summarized in Table I. Obviously, it was found that the calculated values of molar ratios of SIPE/PTA and weight ratios of PEG/PTA were basically consistent with the relative feed values, respectively. According to these ^{1}H-NMR spectra, the molar ratio of DEG/ECDP was also acquired and listed in the table. The presence of DEG can decrease the glass-transition temperature (T_g), melting temperature (T_m) of polymer, and also depress the crystallization and thermal stability of polymers.[5,24]

The Crystalline Structures of CDP and ECDP Samples

WAXD Analysis. Figure 2 shows the WAXD patterns of PET, CDP, and ECDP samples. According to the literature, PET forms a triclinic crystal lattice with the characteristic diffractions at the 2θ angles of 16.3°, 17.5°, 21.6°, 22.9°, 26.1°, and 32.6° assignable to the $(0\bar{1}1)$, (010), $(\bar{1}11)$, $(1\bar{1}0)$, (100), and$(1\bar{1}1)$ planes,[23] respectively. No obvious positional changes of these characteristic diffraction peaks in the WAXD spectra indicated that the added SIPE and PEG units mostly were in the noncrystalline state as minor components in these copolyesters. In other words, the CDP and ECDP copolyesters exhibited the nearly identical crystalline structure to the PET homopolymer. It was

Table I. The Actual Compositions Calculated from ^{1}H-NMR Spectra of Samples

	Feed ratio		Actual composition		
Sample	SIPE/PTA (molar ratio)	PEG/PTA (weight ratio)	SIPE/PTA (molar ratio)	PEG/PTA (weight ratio)	DEG/sample (molar ratio)
PET	–	–	–	–	3.46/100
CDP	3/100	0/100	2.89/100	0/100	4.88/100
ECDP6	3/100	PEG6000/PTA 10/100	2.72/100	8.02/100	5.50/100
ECDP4	3/100	PEG4000/PTA 10/100	2.82/100	8.51/100	5.39/100
ECDP2	3/100	PEG2000/PTA 10/100	2.78/100	8.89/100	4.75/100

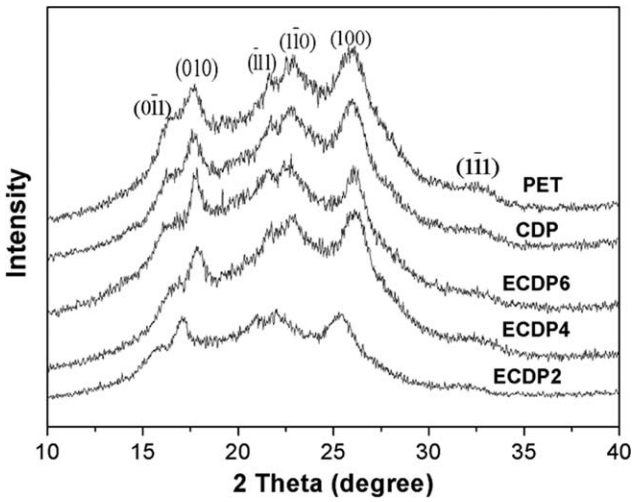

Figure 2. WAXD patterns of PET, CDP, and ECDP samples after the isothermal crystallization processing at 130°C for 60 min.

difficult for SIPE and PEG molecular segments to crowd into crystal lattices and crystalline regions, and the overwhelming molecular chains of them existed in the amorphous regions.[25]

The crystallinity of samples can be obtained by the method of dividing peak.[26] The corresponding crystallinity of PET, CDP, ECDP6, ECDP4, and ECDP2 was 34.05%, 29.54%, 23.39%, 20.61%, and 19.14%, respectively. The crystallinity of CDP sample was lower than that of PET specimen because the effects of polarity of the sulfonated group ($^{-}SO_3Na^{+}$) and steric hindrance of isophthalic structure jointly decreased the regularity of molecular chains. Besides, the crystallinity of ECDP samples was lower than that of CDP specimen since the incorporation of PEG molecular segments increases the irregularity of molecular chain arrangement and leads to more amorphous regions of ECDP samples. In addition, the crystallinity of ECDP samples lessened gradually as the $\overline{M_n}$ of incorporated PEG unit decreased. When the feed weight ratio of PEG/PTA stayed identical (10/100), the lower the $\overline{M_n}$ of PEG unit was, the more molar amounts of PEG molecular segments incorporated into ECDP copolyesters were. Therefore, this caused the ratio of crystalline regions in copolyesters to decrease.

Table II presents the *d*-spacing parameters of PET and its copolyesters gained from WAXD measurements. It was found that all the samples had the similar *d*-spacing values of corresponding crystalline planes, manifesting that the incorporation of SIPE and PEG did not obviously change the *d*-spacing of crystals. The possible reason was that most comonomer segments were in amorphous status, and the alteration of crystal structure was not easily induced by the incorporation of SIPE and PEG units.

SAXS Analysis. All stripe specimens were first uniaxially stretched at different strains along the axial direction for SAXS measurement. Figure 3 shows the SAXS patterns of ECDP6 sample stretched at different strains at room temperature. Figure 3(a) corresponding to the initial sample displayed an incompletely isotropic ring, but a nearly symmetrical rhombus because of a slight orientation.[27] After stretching at different strains, ECDP6 sample illustrated much strong intensity of scattering streak as shown in Figure 3(b–d). It was interpreted that the increase of strain enhanced the regularity of molecular segments along stress direction. Meanwhile, the microvoids in the sample probably appeared because of the stress inducement.

Interestingly, the intensity of scattering streak of ECDP6 sample became weak as the stretching strain was 350% as displayed in Figure 3(c). The increasing strain caused some microcrystals to rearrange and parts of crystal lattices to slip, which together weakened the orientation of molecular chains along stress direction.[27] With the further rising of strain, the scattering streak of ECDP6 sample in Figure 3(d) took on weaker intensity. The possible reason was that the increasing strain caused some crystals to be destroyed, and further deteriorated the arranging regularity of molecular chains.

The 1D SAXS patterns of ECDP6 sample with different strains were illustrated in Figure 3(e). The q denotes the scattering vector, and $q = 4\pi \sin(\theta)/\lambda$, where 2θ is the scattering angle, λ is the wavelength of X-ray.[28] At the beginning stage of stretch, the scattering peak shifted to the lower q value. Upon further stretching, the peak moved back towards the higher q value side. Furthermore, the long period (L) of crystals was calculated from Bragg equation, $L = 2\pi/q^{\star}$, where $q^{\star}$ value is the value of scattering vector corresponding to the scattering peak.[27,28] When the strain was equal to 0%, 200%, 350%, and 500%, the corresponding long period was 10.35, 10.67, 10.50, and 10.39 nm, respectively. The first increasing long period at the strain range of 0–200% could mostly be attributed to the elastic deformation of crystals, the increasing regularity and orientation of molecular chains. Interestingly, the long period decreased when the strain further increased from 200% to 500%. The behavior can explained that the higher strain caused the slippage and fragmentation of some crystals, and lessened the average distance between adjacent lamellae.

Thermal Properties of CDP and ECDP Samples

DSC Analysis. Figure 4 plots the DSC heating curves in the second heating run for CDP and ECDP with different molecular weights of PEG units. The region of glass transition and peaks corresponding to cold crystallization and melting behavior were distinctly exhibited in these curves, and the correlative parameters of thermal property were listed in Table III. It can be observed that the glass-transition temperature (T_g) of ECDP gradually decreased with the fall of PEG molecular weight, but was lower than that of CDP sample. This suggested that the flexibility and irregularity of molecular chains of ECDP samples

Table II. Crystalline Parameters of Samples Obtained from WAXD Measurements

	d-spacing (nm)					
Sample	(0$\bar{1}$1)	(010)	($\bar{1}$11)	($\bar{1}$10)	(100)	(1$\bar{1}$1)
PET	0.53	0.50	0.41	0.38	0.34	0.27
CDP	0.54	0.50	0.41	0.39	0.34	0.27
ECDP6	0.53	0.49	0.41	0.39	0.35	0.28
ECDP4	0.52	0.49	0.40	0.38	0.34	0.27
ECDP2	0.54	0.51	0.42	0.39	0.35	0.28

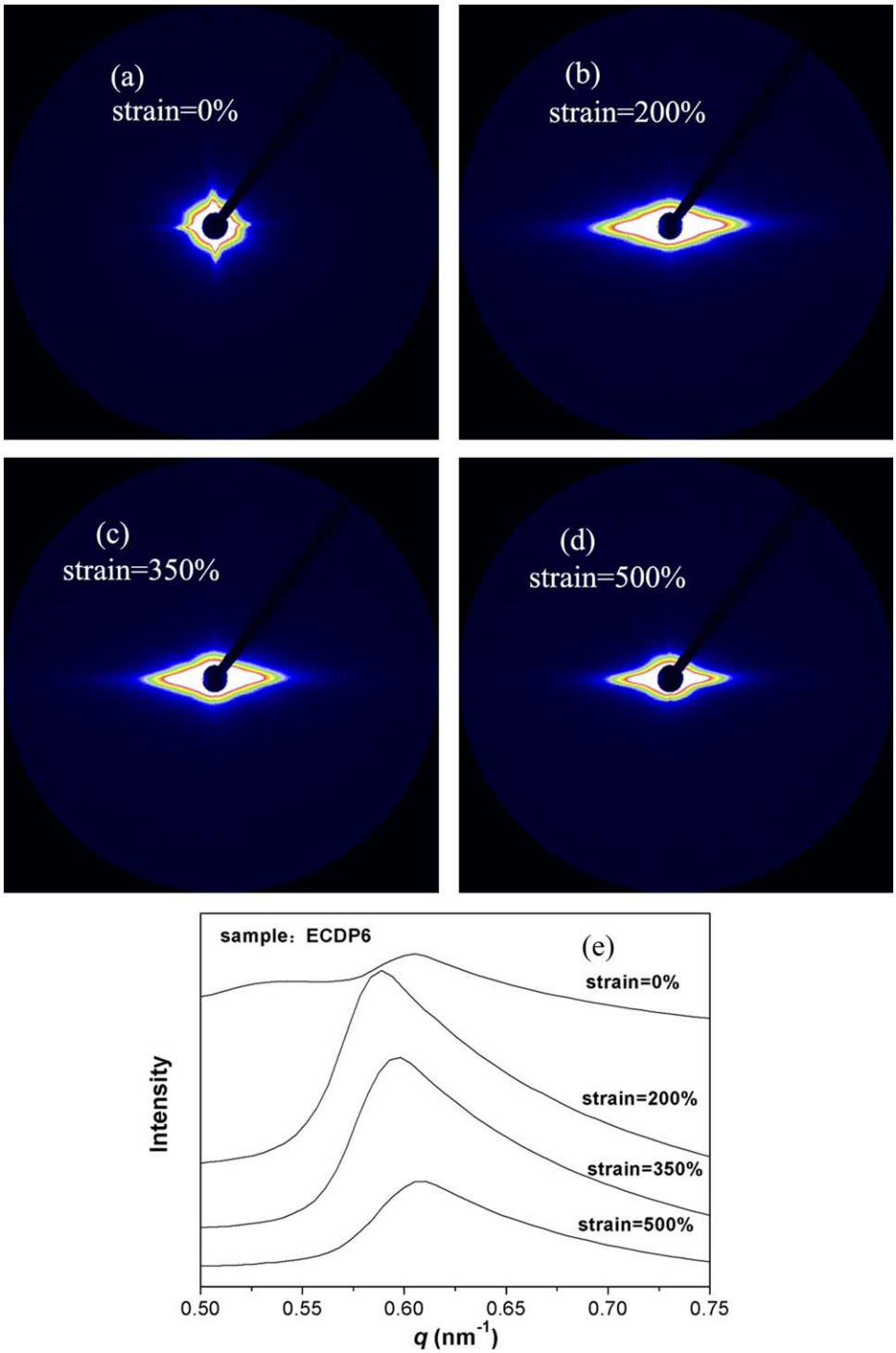

Figure 3. (a) 2D SAXS pattern of ECDP6 sample after being uniaxially stretched (strain = 0%). (b) 2D SAXS pattern of ECDP6 sample after being uniaxially stretched (strain = 200%). (c) 2D SAXS pattern of ECDP6 sample after being uniaxially stretched (strain = 350%). (d) 2D SAXS pattern of ECDP6 sample after being uniaxially stretched (strain = 500%). (e) 1D SAXS patterns of ECDP6 sample after being uniaxially stretched at different strains. [Color figure can be viewed in the online issue, which is available at wileyonlinelibrary.com.]

were enhanced, and their free volume and fraction of amorphous regions increased. Consequently, less energy was needed to make molecular chains moveable. That is to say, the lower T_g these samples have, the better flexibility and soft handling they were endowed with.

Furthermore, the cold-crystallization temperature (T_{cc}) of ECDP gradually reduced when the $\overline{M_n}$ of feed PEG units decreased, meaning that the sample could start to crystallize at lower temperature. It was mostly attributed to the following reason. The incorporation of lower $\overline{M_n}$ of feed PEG units brought more

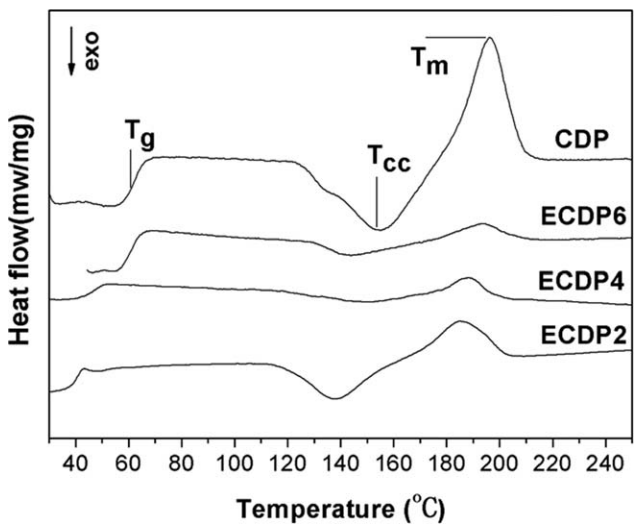

Figure 4. DSC heating curves of CDP and ECDP samples under nitrogen atmosphere.

PEG segments into molecular chains, which resulted into the better flexibility of molecular chains. This enhanced the capability of molecular chains crowding into crystal lattices.

Another thermal parameter of melting temperature (T_m) was found to gradually depress with declining the $\overline{M_n}$ of the feed PEG units. They were mostly because of the incorporation of lower $\overline{M_n}$ of feed PEG units bringing more PEG segments into molecular chains, reducing the arranging regularity of molecular chains, and leading to more amorphous regions and more defective crystalline regions.[29,30]

As the crystalline structure of CDP and ECDP samples was almost identical to the PET homopolymer, the crystallinity (X_c) of these copolyesters was determined by the equation of $X_c = (\Delta H_m/\Delta H_0) \times 100\%$, where ΔH_m is the melting enthalpy of samples, ΔH_0 denotes the melting enthalpy of perfectly crystalline of PET ($\Delta H_0 = 135$ J/g).[31] According to Table III, It was also found that the ΔH_m and X_c of samples gradually decreased as the $\overline{M_n}$ of PEG units reduced, indicating that the incorporation of PEG units weakened the regularity of macromolecular arrangement, decreased the percentage of crystalline regions. Therefore, the crystalline regions tended to be destroyed with less melting enthalpy.

TGA Discussion. Figures 5 and 6 plot the TGA and dTGA curves of CDP and ECDP samples under nitrogen and oxygen atmospheres, respectively. Obviously, the curves seemed to shift towards lower temperature side with the declining of PEG

Table III. The Thermal Parameters of CDP and ECDP Samples Gained from DSC Measurements

Sample	T_g (°C)	T_{cc} (°C)	T_m (°C)	ΔH_m (J/g)	X_c (%)
CDP	61.3	155.1	196.2	37.30	27.63
ECDP6	60.1	151.4	193.5	27.78	20.58
ECDP4	45.7	150.0	188.6	22.71	16.82
ECDP2	40.9	138.2	184.7	21.28	15.76

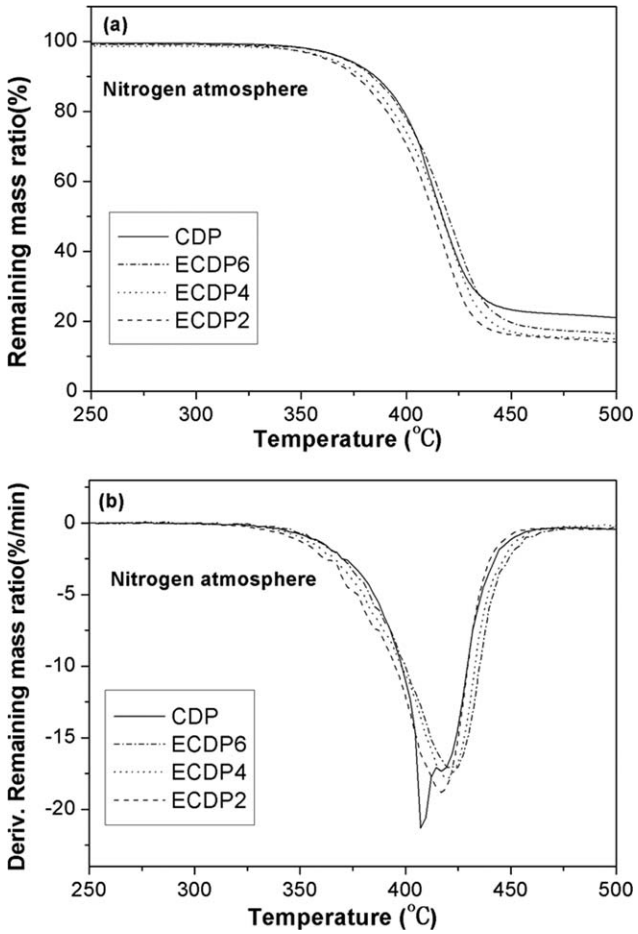

Figure 5. (a) TGA curves of CDP and ECDP samples under nitrogen atmosphere. (b) dTGA curves of CDP and ECDP samples under nitrogen atmosphere.

molecular weight, indicating that the thermal stability of ECDP was deteriorated gradually. Moreover, the TGA curves of CDP and ECDP samples under nitrogen atmosphere were found to have only one weight-loss stage, which was confirmed for the single peak in the dTGA curves of samples. Comparatively, the TGA curves under oxygen atmosphere owned two weight-loss stages corresponding to the two peaks in the dTGA curves. The first weight-loss stage was mainly attributed to the thermal degradation process of macromolecules owning long molecular chains and huge molecular weight breaking into shorter molecular chain fragments via the chain scission when samples were gradually heated up to a certain high temperature.[32] Subsequently, these fragments could be further thermal-oxidized into many smaller volatile products and solid residues after several steps because of the existence of oxygen.[24,33–35]

According to the above curves, some useful parameters such as the onset temperature (T_{onset}), mass loss rate, and corresponding temperature were acquired as summarized in Table IV. The degradation temperatures of CDP and ECDP samples corresponding to different mass losses were found to reduce with the decreasing $\overline{M_n}$ of feed PEG units. The reasons could be elucidated as followed. The PEG units with low $\overline{M_n}$ meant the more PEG segments were incorporated into the main molecular

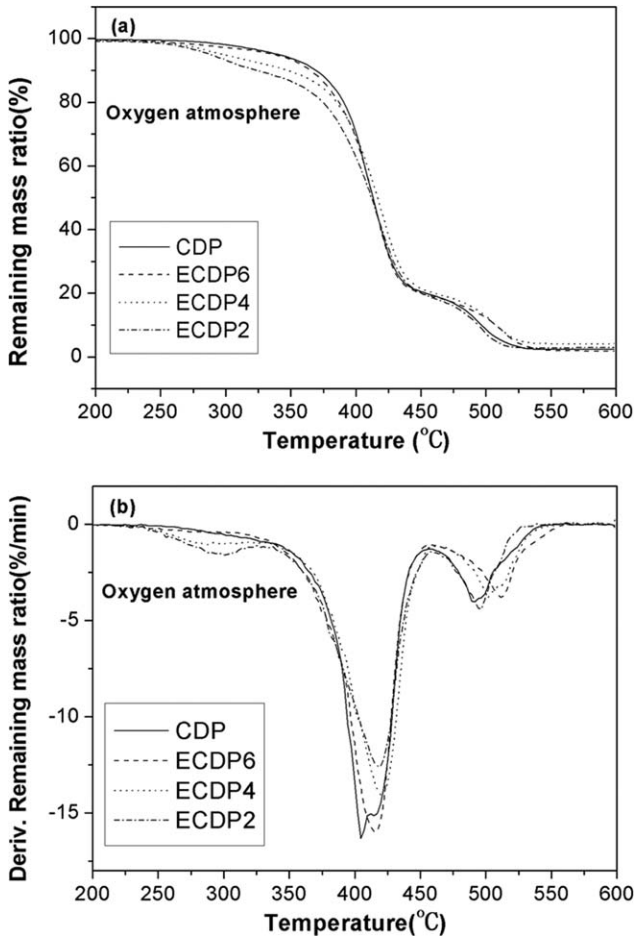

Figure 6. (a) TGA curves of CDP and ECDP samples under oxygen atmosphere. (b) dTGA curves of CDP and ECDP samples under oxygen atmosphere.

chains, so the ether bond (—o—) distribution in the main molecular chains was widened. In addition, the ether bonds enhanced the electronegativity of oxygen atom in the ester carbonyl, and increased the electropositivity of hydrogen atom in the methylene of β positon.[36] Therefore, it was more prone to rupture for correlative bonds (C=O and CH—H) and easily break at weak bonds (CH2—O) in copolyesters, and then the

Table IV. Degradation Temperatures of CDP and ECDP Samples Corresponding to Different Mass Losses Under Nitrogen and Oxygen Atmosphere

	Mass loss rate(%) and corresponding temperature(°C)					
	Under nitrogen atmosphere			Under oxygen atmosphere		
Sample	Onset	30%	50%	Onset	30%	50%
CDP	394.9	406.6	417.3	385.7	402.3	416.7
ECDP6	388.6	400.5	413.5	384.8	400	413.1
ECDP4	387.1	398.6	410	381.6	399.4	412.7
ECDP2	385.5	394.0	405.1	371.5	391.8	412

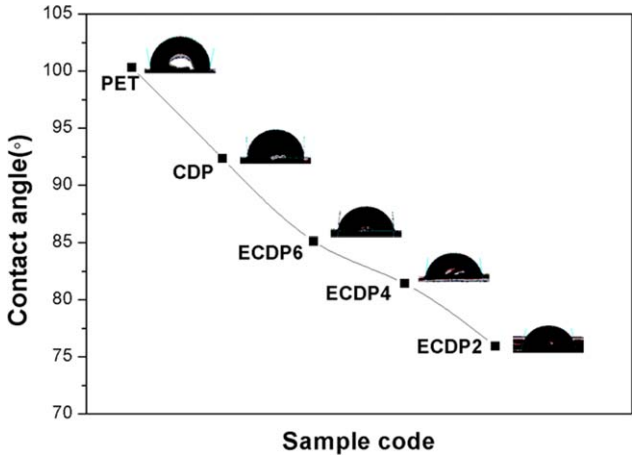

Figure 7. Variation of the contact angles of PET, CDP, and ECDP samples. [Color figure can be viewed in the online issue, which is available at wileyonlinelibrary.com.]

new free radicals and end groups were produced, which led to the thermal degradation to occur more easily.[35] The above pyrolysis process can concisely be depicted as in Scheme 1.[24]

Another case should be pointed out that, compared with the thermal degradation under nitrogen atmosphere, the characteristic degradation temperature was lower under oxygen conditions. This was because it was easier for the ether bonds in copolyesters to break up, and resulted in the occurrence of the thermal degradation under the reactive oxygen atmosphere.

Analysis of the Contact Angle of Samples

The contact angle is an important parameter, which can characterize the hydrophilicity of copolyesters. The smaller the value of contact angle is, the better the hydrophilicity is.[37] Figure 7 displays the contact angles of PET, CDP, and ECDP samples with different $\overline{M_n}$ of PEG units. PET was found to have higher value contact angle than CDP sample, indicating that its hydrophilicity was worse than the latter. It can be explained that the introduction of SIPE unit into the CDP molecular chains brings the negative dye sites (sulfonated group) and decreases the regularity of molecular chain arrangement. Besides, the value of contact angle of CDP sample was higher than that of all the ECDP samples. It shows that the hydrophilicity of ECDP is superior to that of CDP because the incorporation of PEG segments increases the content of ether bonds and the irregularity of molecular chain arrangement, and results in more amorphous regions. Additionally, the values of contact angle of ECDP samples were found to gradually decrease as the $\overline{M_n}$ of feed PEG unit decreased, meaning that the hydrophilicity of ECDP samples was improved. The incorporation of lower $\overline{M_n}$ of feed PEG units brings more PEG molecular segments into molecular chains, and produces the new free radicals and hydroxyl endgroups, and reduces the regularity of molecular chain arrangement, which is helpful to reinforce the polymeric hydrophilicity.[38]

CONCLUSIONS

CDP and ECDP copolyesters based on PET were prepared with SIPE and PEG units with different molecular weights as modifiers. NMR results showed that the actual molar ratio of PTA :

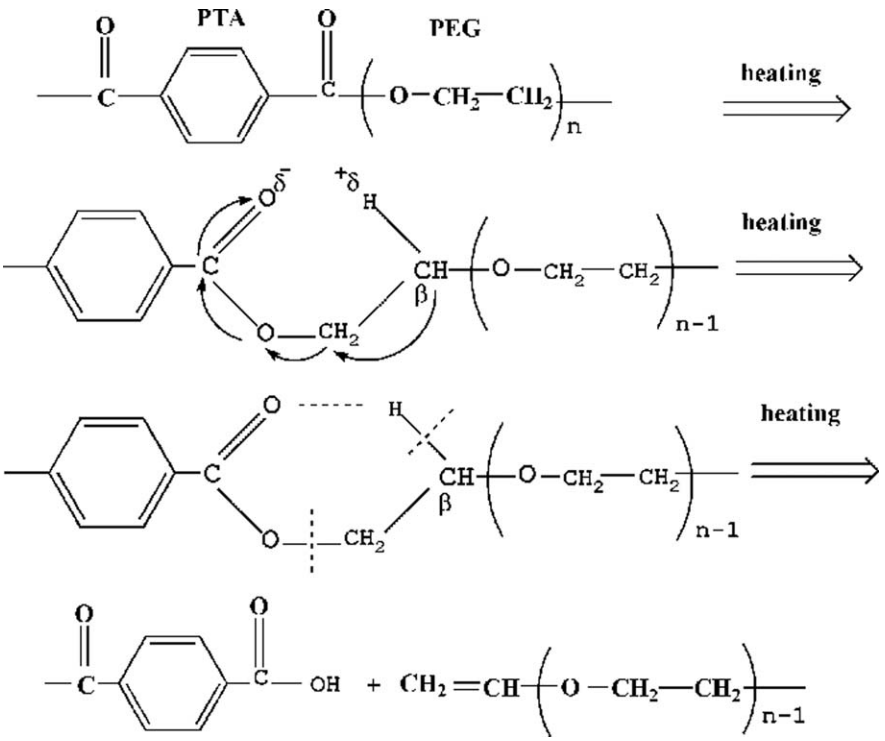

Scheme 1. The concise depiction of mechanism of thermal degradation process of ECDP samples.

PEG : SIPE was basically accordant with the relative feed ratio. WAXD results showed that the crystalline structures of CDP and ECDP samples were similar to that of PET and the crystallinities gradually reduced with the decrease of the $\overline{M_n}$ of feed PEG units, which suggested that molecular chains of SIPE and PEG units overwhelmingly existed in the amorphous region. SAXS results showed that lower strain enhanced the orientation, whereas a certain higher strain tended to deteriorate the orientation of molecular chains. The long period firstly increased at the strain range of 0–200%, whereas it decreased as the strain further increased from 200% to 500%. Furthermore, thermal properties of these copolyesters under different conditions were characterized by DSC and TGA. Experimental results indicated that their T_g, T_{cc}, T_m, and T_{onset} gradually reduced with the decreasing $\overline{M_n}$ of PEG units, because the incorporation of lower $\overline{M_n}$ of PEG units brought more ether bonds into molecular chains and increased the irregularity of molecular chains. The results also indicated that the thermal degradation under oxygen conditions happened easily compared to that under nitrogen conditions. The TGA curves under nitrogen atmosphere had only one weight-loss stage, whereas the curves under oxygen atmosphere owned two weight-loss stages. Contact angle results indicated that the values of contact angle lessened with decreasing the $\overline{M_n}$ of feed PEG units. That is to say, the hydrophilicity was better when the $\overline{M_n}$ of feed PEG units decreased, as the incorporation of lower $\overline{M_n}$ of PEG units led to more amorphous regions and increased ether bond and hydroxyl groups in the molecular chains.

ACKNOWLEDGMENTS

This work is supported by National "Twelfth Five-Year" Science and Technology Support Program of China: The Key Manufacturing Technique Development of New Polyester Cotton-like Fibers (No.2011BAE05B04), and the Fundamental Research Funds for the Central Universities (No. 12D10143).

REFERENCES

1. Kiziltas, A.; Gardner, D. J.; Han, Y.; Yang, H. -S. *J. Therm. Anal. Calorim.* **2011**, *103*, 163.
2. Tang, S.; Xin, Z. *Polymer* **2009**, *50*, 1054.
3. Bech, L.; Meylheuc, T.; Lepoittevin, B.; Roger, P. *J. Polym. Sci. Polym. Chem.* **2007**, *45*, 2172.
4. Wei, G. F.; Wang, L. Y.; Chen, G. K.; Gu, L. X. *J. Appl. Polym. Sci.* **2006**, *100*, 1511.
5. Kint, D. P. R.; Munoz-Guerra, S. *Polym. Int.* **2003**, *52*, 321.
6. Bouma, K.; Regelink, M.; Gaymans, R. J. *J. Appl. Polym. Sci.* **2001**, *80*, 2676.
7. Zhou, C.; Zhang, H.-W.; Jiang, Y.; Wang, W.-J.; Yu, Q. *J. Appl. Polym. Sci.* **2011**, *121*, 1254.
8. Akkaya, A.; Pazarlioglu, N. K. *J. Appl. Polym. Sci.* **2011**, *121*, 690.
9. Tsenoglou, C. J.; Kiliaris, P.; Papaspyrides, C. D. *Macromol. Mater. Eng.* **2011**, *296*, 630.
10. Dadashian, F.; Montazer, M.; Ferdowsi, S. *J. Appl. Polym. Sci.* **2010**, *116*, 203.
11. Inagaki, N.; Narushim, K.; Tuchida, N.; Miyazaki, K. *J. Polym. Sci. Polym. Phys.* **2004**, *42*, 3727.
12. Dadsetan, M.; Mirzadeh, H.; Sharifi-Sanjani, N. *J. Appl. Polym. Sci.* **2000**, *76*, 401.
13. Lee, M. S.; Lee, M.; Wakida, T.; Saito, M.; Yamashiro, T.; Nishi, K.; Inoue, G.; Ishida, S. *J. Appl. Polym. Sci.* **2007**, *104*, 2423.

14. Eisenberg, A.; Hird, B.; Moore, R. B. *Macromolecules.* **1990**, *23*, 4098.
15. Pal, S. K.; Gandhi, R. S.; Kothari, V. K. *J. Appl. Polym. Sci.* **1996**, *61*, 401.
16. Liu, L.; Cheng, L.; Yu, J.; Xie, H. *J. Appl. Polym. Sci.* **2011**, *120*, 195.
17. Hsiao, K. -J.; Kuo, J. -L.; Tang, J. -W.; Chen, L. -T. *J. Appl. Polym. Sci.* **2005**, *98*, 550.
18. Guo, X. Y.; Gu, L. X.; Feng, X. X., *J. Appl. Polym. Sci.* **2002**, *86*, 3660.
19. Finelli, L.; Fiorini, M.; Siracusa, V.; Lotti, N.; Munari, A. *J. Appl. Polym. Sci.* **2004**, *92*, 189.
20. Imran, M.; Kim, B. -K.; Han, M.; Cho, B. G.; Kim, D. H. *Polym. Degrad. Stabil.* **2010**, *95*, 1688.
21. Chaouch, W.; Dieval, F.; Le Nouen, D.; Defoin, A.; Chakfe, N.; Durand, B. *J. Biomed. Mater. Res. A.* **2009**, *91*, 943.
22. Yue, Q. F.; Wang, C. X.; Zhang, L. N.; Ni, Y.; Jin, Y. X. *Polym. Degrad. Stabil.* **2011**, *96*, 401.
23. Chen, B.; Gu, L. *J. Appl. Polym. Sci.* **2010**, *117*, 2456.
24. Nayak, S.; Labde, J.; Geedh, S.; Jaisingh, S. K.; Rao, K.; Venkatachalam, S.; Kelkar, A. K. *J. Appl. Polym. Sci.* **2010**, *118*, 2797.
25. Wang, Z. G.; Hsiao, B. S.; Fu, B. X.; Liu, L.; Yeh, F.; Sauer, B. B.; Chang, H.; Schultz, J. M. *Polymer* **2000**, *41*, 1791.
26. Jiang, G.; Huang, W.; Li, L.; Wang, X.; Pang, F.; Zhang, Y.; Wang, H., *Carbohyd. Polym.* **2012**, *87*, 2013.
27. Zuo, F.; Keum, J. K.; Chen, X.; Hsiao, B. S.; Chen, H.; Lai, S. -Y.; Wevers, R.; Li, J. *Polymer.* **2007**, *48*, 6867.
28. He Y.; Zhu B.; Kai WH.; Inoue Y. *Macromolecules.* **2004**, *37*, 3341.
29. Varma, D. S.; Maheswari, A.; Gupta, V.; Varma, I. K. *Die. Angew. Makromol. Chem.* **1980**, *90*, 23.
30. Wang, C.; Zhang, Z.; Mai, K. *J. Therm. Anal. Calorim.* **2011**, *106*, 898.
31. Shieh, YT.; Lin, YS.; Twu, YK.; Tsai, HB.; Lin, RH. *J. Appl. Polym. Sci.* **2010**, *116*, 1336.
32. Przepiorski, J.; Karolczyk, J.; Tsumura, T.; Toyoda, M.; Inagaki, M.; Morawski, A. W. *J. Therm. Anal. Calorim.* **2012**, *107*, 1150.
33. Li, X. -G.; Huang, M. -R.; Bai, H., *Die. Angew. Makromol. Chem.* **1998**, *256*, 13.
34. Li, F. X.; Xu, X. J.; Li, Q.; Li, Y.; Zhang, H. Y.; Yu, J. Y.; Cao, A. M. *Polym. Degrad. Stabil.* **2006**, *91*, 1688.
35. Nait-Ali, L. K.; Colin, X.; Bergeret, A., *Polym. Degrad. Stabil.* **2011**, *96*, 240.
36. Wei, G.; Hua, D.; Gu, L. *J. Appl. Polym. Sci.* **2006**, *101*, 3334.
37. Zhang, H. W.; Du, Z. Y.; Jiang, Y.; Yu, Q. *J. Appl. Polym. Sci.* **2012**, *126*, 1950.
38. Montarsolo, A.; Varesano, A.; Mossotti, R.; Rombaldoni, F.; Periolatto, M.; Mazzuchetti, G.; Tonin, C. *J. Appl. Polym. Sci.* **2012**, *126*, 1388.